Physics of Fluids

RESEARCH ARTICLE | AUGUST 11 2026

Increasing cooling efficiency with electric field and feedback

A. L. Kupershtokh ; D. A. Medvedev ; A. V. Alyanov

Physics of Fluids 38, 083328 (2026)
https://doi.org/10.1063/5.0345251

Physics of Fluids ARTICLE pubs.aip.org/aip/pof

Increasing cooling efficiency with electric field and feedback

Cite as: Phys. Fluids **38**, 083328 (2026); doi: 10.1063/5.0345251
Submitted: 26 May 2026 · Accepted: 27 July 2026 ·
Published Online: 11 August 2026

View Online Export Citation CrossMark

A. L. Kupershtokh,[a] D. A. Medvedev, and A. V. Alyanov

AFFILIATIONS

Lavrentyev Institute of Hydrodynamics of SB RAS, 630090 Novosibirsk, Russia

[a]Author to whom correspondence should be addressed: skn@hydro.nsc.ru

ABSTRACT

In this article, we present mesoscopic simulations of the fluid flow and heat transfer in a model of a heat pipe with the action of a non-uniform electric field on the fluid, based on the lattice Boltzmann method. We demonstrate in numerical experiments the possibility to realize the controlled quasiperiodic flow of a film of dielectric liquid in the vicinity of a non-conductive inset using the cyclic change of the electric field and the regularly switching flow of liquid condensed in the cold section back to the cooled hot surface. We model the process of the pulse action of a non-uniform electric field on the liquid film with a feedback based on the thickness of the liquid films at the cooling region and at the vapor condenser. Such combined action ensures the increased average value of the heat flux from the heater. In our experiments, the value of the heat flux was 1.7 times higher than the heat flux without the electric field for the same geometry of the region, the same temperatures, and the same amount of the cooling fluid.

I. INTRODUCTION

In microfluidics and microelectronics, it is necessary to cool heated surfaces to prevent them from overheating. For this purpose, evaporation of liquid films or many droplets is widely used (rivulet or spray cooling).[1–4] The effectiveness of such methods is ensured by the intensive evaporation of the liquid surface and its cooling due to the absorption of the latent heat of the phase transition. One of the ways to remove vapor from the cooled surface is the process used in so-called "heat pipes," where vapor condenses at a special part of the tube with a lower temperature, and then the liquid returns to the cooled surface.[5–9]

It is commonly assumed that the cooling of heated surfaces by evaporating liquid droplets or films is more effective when numerous contact lines are present.[10–15] However, the generation of contact lines inevitably leads to the occurrence of dry spots at the surface. The heat flux from these spots is essentially lower. It was shown in Refs. 16 and 17 that this leads to a decrease in the total heat removal from the surface.

In Refs. 18–20, the principal possibility of the rupture of liquid films under the action of non-uniform electric fields and the process of the generation of contact lines by the perforation of thin films of dielectric liquid placed on the electrode surface was demonstrated. A non-uniform electric field was produced at the edges of solid non-conductive insets in a segmented flat electrode.

It was proposed in Ref. 17 to intensify the heat exchange process on solid surfaces at the mini- and microscale by decreasing the thickness of the evaporating film without its rupture. For this purpose, the possibility of using periodic voltage pulses was suggested in Ref. 17. In order to avoid the film rupture a regular inflow of liquid to the working film is necessary. In the present article, we realize such a possible process of the pulse action on the liquid film with a feedback that ensures an increase in the average value of the heat removal from the heater. One of the purposes of this article is precisely to draw the attention of experimenters to this phenomenon.

The paper is organized in the following way. In Sec. II, we describe briefly the lattice Boltzmann method (LBM) applied to simulate the motion of fluid, phase transitions, and convective heat transport. Section III is devoted to the description of the cooling process by the evaporating liquid film, and the influence of non-uniform electric field on this process. In Sec. IV, we introduce the feedback setup, which allows us to prevent the breakup of the film and to get the increased average heat flux. Simulation results are presented in Sec. V. Finally, the summary is given in the Conclusion section.

II. LATTICE BOLTZMANN METHOD

Lattice Boltzmann method (LBM) is widely used to simulate fluid flows with phase transitions. The authors of the present article have made significant contribution into the application of LBM for simulation of electrohydrodynamic flows and flows with heat transport.[21–26]

In LBM, the fluid flow is described by solving the Boltzmann kinetic equation with a discrete set of particle velocities $\mathbf{c}_k$, which should correspond to the lattice vectors $\mathbf{e}_k = \mathbf{c}_k\Delta t$. One-particle distribution functions $f_k, k = 0, \ldots, m$ are used as main variables. Their evolution equation has the form

$$f_k(\mathbf{x} + \mathbf{c}_k\Delta t, t + \Delta t) = f_k(\mathbf{x}, t) + \Omega_k\{f_k\} + \Delta f_k. \quad (1)$$

Fluid density ρ and mass velocity $\mathbf{u}$ are calculated as the moments of distribution functions,

$$\rho = \sum_{k=0}^{m} f_k \quad \text{and} \quad \rho\mathbf{u} = \sum_{k=0}^{m} f_k\mathbf{c}_k. \quad (2)$$

Characteristics of the LBM are the straight lines corresponding to the directions of the velocity vectors $\mathbf{c}_k$; the values of the distribution functions f_k propagate along these lines.

In this work, the collision operator in the form of relaxation to locally equilibrium values is used,

$$\Omega_k\{f_k\} = (f_k^{eq}(\rho, \mathbf{u}) - f_k(\mathbf{x}, t))/\tau, \quad (3)$$

with single non-dimensional relaxation time τ (LBGK model[27]) Here, f_k^{eq} are the equilibrium values of the distribution functions.[28]

Change of the distribution functions due to the action of forces is taken into account using the exact difference method (EDM),[21–24]

$$\Delta f_k = f_k^{eq}(\rho, \mathbf{u} + \Delta\mathbf{u}) - f_k^{eq}(\rho, \mathbf{u}), \quad (4)$$

where the velocity change during one time step $\Delta\mathbf{u}$ depends on the total force $\mathbf{F}$ acting on the fluid at a node $\Delta\mathbf{u} = \mathbf{F}\Delta t/\rho$. This method is included in several international computer modeling packages: LBsoft, OpenLB, DL-MESO, XLB-libr, HyLBM, and JAX-Lab. In this case, the physical fluid velocity should be calculated at half time step,[29]

$$\rho\mathbf{u}^* = \sum_{k=0}^{m} f_k\mathbf{c}_k + \mathbf{F}\Delta t/2. \quad (5)$$

The pseudopotential method[30] is used to simulate phase transitions. The total force $\mathbf{F}$ acting on the fluid at a node is expressed as

$$\mathbf{F} = -\nabla U, \quad (6)$$

where the pseudopotential U is expressed using the equation of state for the fluid $U = P(\rho, T) - \rho\theta$. Here, $\theta = (h/\Delta t)^2/3$ is the kinetic temperature, h is the lattice spacing. This method provides the separation of the liquid and the gas phases as well as the surface tension at the boundary between phases and its temperature dependence. The formula (6) can be conveniently rewritten in the mathematically equivalent form introducing the function $\Phi = \sqrt{-U}$ (see Ref. 23)

$$\mathbf{F}(\mathbf{x}) = 2A\nabla(\Phi^2) + (1 - 2A)2\Phi\nabla\Phi. \quad (7)$$

The free parameter A is chosen such that to obtain the best agreement between the calculated coexistence curve liquid-vapor and the theoretical one obtained from the equation of state. For the van der Waals equation of state used in this work, the value is $A = -0.152$ (see Ref. 23).

To simulate the action of fluid with solid walls, the commonly used bounce-back boundary conditions (no-slip boundaries) are applied for f_k. The wetting of walls is simulated using the method by setting the values of pseudopotential in boundary nodes in the same way as described in Ref. 17. Formally, the contact angle was assumed to be equal to 90° (neutral wetting).

The convective heat transport is simulated using the additional set of distribution functions g_k with the evolution equation in the form[25]

$$g_k(\mathbf{x} + \mathbf{c}_k\Delta t, t + \Delta t) = g_k(\mathbf{x}, t) + \frac{g_k^{eq}(\rho, \mathbf{u}) - g_k(\mathbf{x}, t)}{\tau_W} + \Delta g_k, \quad (8)$$

where τ_W is the non-dimensional relaxation time for the internal energy. The internal energy per unit volume is equal to

$$W = \sum_{k=0}^{m} g_k. \quad (9)$$

The conductive heat transport and the pressure work are calculated using an explicit finite-difference scheme.

For fluid with the van der Waals equation of state,

$$P = \frac{\rho RT}{1 - b\rho} - a\rho^2, \quad (10)$$

the internal energy per unit mass is equal to $e = C_V T - a\rho$, where C_V is the specific heat at constant volume. The heat of the phase transition is the change of the internal energy when the fluid density changes from the density of liquid ρ_L to the density of vapor ρ_V (plus the work against pressure which is taken into account separately). At constant temperature, the latent heat of evaporation is equal to

$$Q = e_V - e_L = a(\rho_L - \rho_V). \quad (11)$$

The temperature dependence of the latent heat $Q(T)$ is taken into account implicitly through the temperature dependence of ρ_L and ρ_V at the phase coexistence curve.

For the change of the internal energy per unit volume due to the phase transition in a cell inside the transition layer, one obtains[26]

$$\frac{dW}{dt} = \frac{\rho_L Q(T)}{\rho_L - \rho_V}\frac{d\rho}{dt}. \quad (12)$$

It is assumed that the evaporation heat $Q(t)$ is absorbed or released in the range of density $[\rho_V, \rho_L]$. Then, taking into account Eq. (11), we get the following equation:

$$\frac{dW}{dt} = a\rho_L\frac{d\rho}{dt} = -a\rho_L \operatorname{div}\mathbf{u}^*. \quad (13)$$

For the density, the pressure, and the temperature, we use the values reduced by the critical ones. The non-dimensional variables are $\tilde{P} = P/P_c, \tilde{T} = T/T_c, \tilde{\rho} = \rho/\rho_c$ (here, P_c, T_c, ρ_c are the critical values). Equation (10) takes the form

$$\tilde{P} = \frac{8\tilde{\rho}\tilde{T}}{3 - \tilde{\rho}} - 3\tilde{\rho}^2, \quad (14)$$

and the non-dimensional heat of evaporation is equal to $\tilde{Q} = 3(\tilde{\rho}_L - \tilde{\rho}_V)$. Lattice units are used for the spatial and the

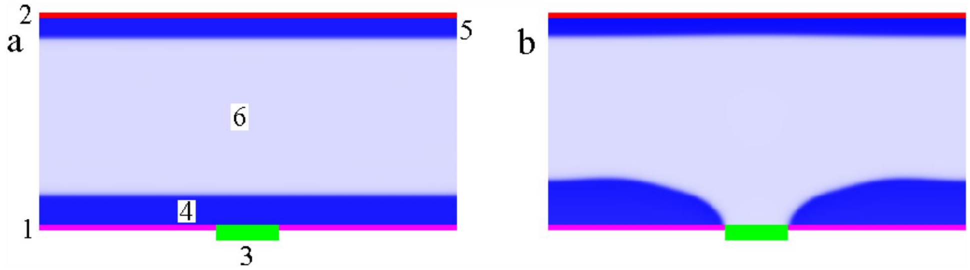

FIG. 1. (a) Initial state before the switch-on of heating and electric field at $t = 5000$. (b) Breakup of film without the switch-off of the electric field $t = 19\,000$. 1—lower electrodes, 2—upper electrode, 3—solid non-conductive inset, 4—liquid film on the heater, 5—liquid film on the condenser, 6—vapor. Width of the non-conductive inset is $2R_{in} = 60$. Size of the calculation domain is 400×200.

temporal scales. The relaxation times for the fluid and for the internal energy are $\tau = 1, \tau_W = 0.53$.

III. NUMERICAL MODEL OF THE COOLING PROCESS

A mesoscopic numerical model based on the LBM is developed for simulating the non-stationary fluid flows of dielectric liquids with phase boundaries under the action of a non-uniform electric field on the fluid. Gravity, surface tension, heat transport, evaporation of liquid, and condensation of vapor are taken into account.

The principal setup of the cooling system[17] is shown in Fig. 1(a). A film of dielectric liquid is placed on the hot lower conductive surface (electrode). The evaporation of this film cools the heater. There is a non-conductive inset in the central part of the lower electrode. The thickness of the liquid film above the center of this inset is denoted as $h_1(t)$. The vapor condenses at the cold upper electrode producing the liquid film of thickness $h_2(t)$. The lower electrode is electrically grounded, and the voltage V is applied to the upper electrode. After the application of voltage, a non-uniform electric field is generated near the edges of the non-conductive inset. The Helmholtz volume force[31]

$$\mathbf{F} = -\frac{\varepsilon_0 E^2}{2}\,\mathrm{grad}\,\varepsilon + \frac{\varepsilon_0}{2}\,\mathrm{grad}\left[E^2\rho\left(\frac{\partial\varepsilon}{\partial\rho}\right)_T\right] \tag{15}$$

pulls the dielectric liquid into the regions of stronger electric field. Here, ε_0 is the electrostatic constant, E is the magnitude of the electric field, ε is the permittivity of the fluid. This leads to the decrease in the film thickness above the non-conductive inset and to the increase in the heat flux through the film. Increasing heat flux intensifies the evaporation. The distribution of the electric potential φ in the dielectric fluid is obtained by solving the Poisson's equation $\mathrm{div}(\varepsilon\mathrm{grad}\varphi) = 0$. At the surface of the dielectric inset, the normal derivative of the electric potential is set to zero, that can be used if permittivity of solid non-conductive inset is equal to permittivity of the liquid film. The periodic boundary conditions are used for side boundaries.

In order to characterize the relative strength of the electric field, it was suggested in Refs. 19 and 20 to use the modified definition of the electric Bond number, namely, $\mathrm{Bo}_E^* = \varepsilon_0(\varepsilon_L - 1)E_0^2 R_{in}^2/(\delta\varepsilon_L\sigma)$. This quantity depends both on the initial film thickness δ and on the radius (or half-width) of the non-conductive inset R_{in}. Here,

$$E_0 = \frac{\varepsilon_L V}{\varepsilon_L h - (\varepsilon_L - 1)\delta}$$

is the initial electric field strength above the film surface, ε_L is the permittivity of liquid, and h is the interelectrode distance.

It was shown in Refs. 16 and 17 that the heat flux decreases after the film breakup [Fig. 1(b)] despite the appearance of new contact lines with enhanced heat flux in their vicinity. Even when the electric field was switched off beforehand, the breakup finally occurred because of the continuing film evaporation and, correspondingly, the overall decrease in its thickness.

IV. SIMULATION OF THE COOLING PROCESS WITH FEEDBACKS

We simulate the quasiperiodic flow of the film in the vicinity of the non-conductive inset controlled by the regularly changed electric field.

In order to compensate for the continued evaporation of the film and the decrease in its thickness, the following variant to organize the flow of fluid is proposed (Fig. 2).

In order to realize the quasiperiodic regime of heat removal when the film thickness changes in a certain range, it is necessary to switch the electric field on and off at certain prescribed values of the film thickness h_1 above the center of the non-conductive inset. We chose the range between 10 and 17 lattice units. The breakup of the

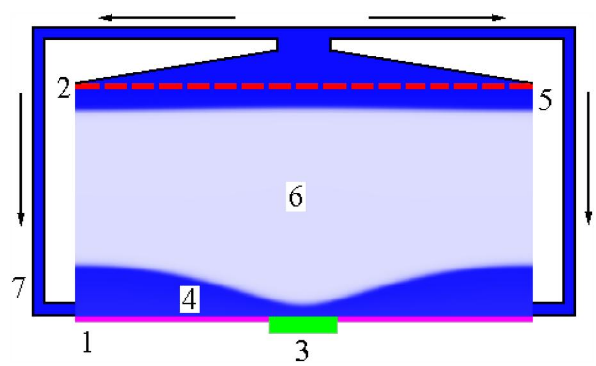

FIG. 2. Setup for the cooling of a heater. 1 and 2—lower and upper electrodes, 3—non-conductive inset, 4 and 5—liquid films at the heater and at the condenser, 6—vapor, 7—channels for backflows. Size of the calculation domain between electrodes is 400×200.

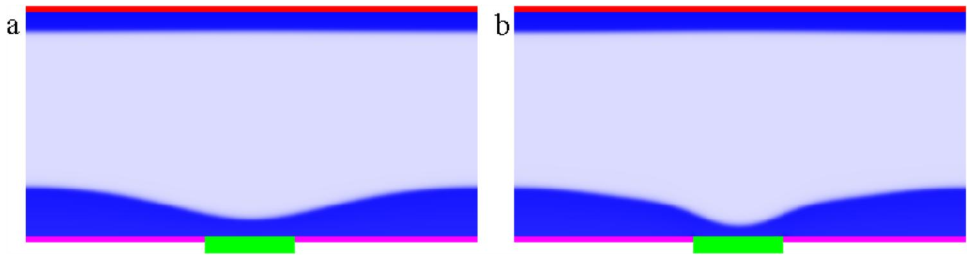

FIG. 3. Film thickness above the center of the non-conductive inset decreases rapidly from 17 lattice units at $t = 22\,384$ (a) to ten lattice units at $t = 24\,920$ (b) after the next switch-on of the field. Electric field is switched on for the first time at $t = 5000$. $2R_{in} = 80$, $T_h = 0.75$.

film does not occur for such a regime of switching the electric field with the feedback on the film thickness $10 \le h_1 \le 17$. The instantaneous film thickness is determined by the position of the isosurface $\rho = 1$ inside the transition layer between liquid and vapor.

Evaporated dielectric liquid condenses at the cold upper electrode. A part of this condensate needs to be fed back into the liquid film on the heater, which cools the hot surface by evaporation. The scheme of the fluid flows in such a closed system is shown in Fig. 2.

To accomplish this, the liquid is removed uniformly from the base of the film (5) through the porous upper electrode (2). Then, the removed liquid is fed back through the bypass channels (7) to the sides of the working film (4) in a layer of prescribed thickness adjacent to the lower electrode (Fig. 2). In this paper, the thickness of this layer was set to ten lattice units. In the model, such a process is simulated by setting corresponding boundary conditions at the upper and side boundaries of the calculation domain.

The velocity boundary conditions are used in the form proposed in Refs. 32 and 33. Here, the values for distribution functions f_{in} for the characteristics entering the computation area are set by the multiplication of the values for the outcoming characteristics f_{out} by a certain coefficient β, which depends on the local fluid velocity u at the boundary,

$$\beta = \frac{1 - 3u + 3u^2}{1 + 3u + 3u^2}. \tag{16}$$

Zero flux corresponds to the value $\beta = 1$. At the side boundaries, this gives $f_{in}(0, j) = \beta_1 f_{out}(1, j)$ and $f_{in}(nx + 1, j) = \beta_1 f_{out}(nx, j)$. At the upper boundary, we have $f_{in}(i, ny + 1) = \beta_2 f_{out}(i, ny)$. Here, nx and ny are, correspondingly, the width and the height of the calculation domain. In the most part of calculations, one and the same value $\beta_2 = 0.998$ was used for the whole upper boundary, which corresponds to the uniform outflow of liquid with the velocity $u_2 \approx 0.000\,33$ lattice units. The condition of mass conservation should be satisfied, i.e., the outflow velocity at the upper boundary u_2 and inflow velocity to the lower layer u_1 (the values of β_1 and β_2) should be adjusted such that $\rho_1 u_1 S_1 = \rho_2 u_2 S_2$. Here, S_1 and S_2 are the cross sections for the inflow and the outflow of liquid.

The above-described scheme of fluid flows corresponds to the so-called "loop heat pipes," the idea of which was proposed in Refs. 7 and 8. The difference is that we realized a precise feedback for the flow of liquid from the vapor condenser to the cooling film in order to maintain the fixed range of the film thickness at the upper electrode ($17 \le h_2 \le 21$), similar to switching the electric field on and off. These procedures provide the cyclic cooling process.

V. SIMULATION RESULTS

The initial temperature of the fluid in the system was set to $T_0 = 0.7$. The temperature of the heater is fixed to $T_h = 0.7$ or $T_h = 0.75$, and the temperature of the vapor condenser was $T_c = 0.6$. The electric field is first turned on at time $t = 5000$. After the application of voltage, the film thickness above the center of the non-conductive inset decreases from $h_1 = \delta = 30$ to $h_1 = 10$ lattice units (Fig. 4). Afterward, the electric field is turned off.

After the next switch-on of the field, the film thickness above the center of the non-conductive inset decreases rapidly from 17 to 10 lattice units [Figs. 3(b) and 4]. The backflow of liquid into the deepening in the film on the heater after the beginning of the feeding of liquid is a much slower stage.

Thus, in order to provide the quasiperiodic regime of cooling, feedback is realized between the thickness of liquid films, the switch-on of the electric field, and the backflow of liquid between films.

Figure 4 shows the time dependence of the total heat flux from the heater after the switch-on of the automatic regime (red curve). The diagrams of switching of the electric field E_{on} and the liquid backflow from the condenser to the cooling layer F_{on} are also presented. After several field switching cycles, the system achieves a quasiperiodic regime with an approximately constant average value of the heat flux $Q_{aver} \approx 24$. In this regime, the voltage pulses are applied

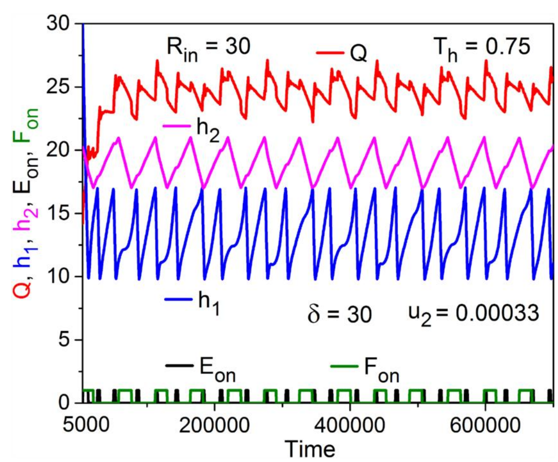

FIG. 4. Total heat flux from the heater Q. Electric field is switched on for the first time at $t = 5000$. $2R_{in} = 60$, $\mathrm{Bo}_E^* = 2.5$, $T_h = 0.75$, $u_2 \approx 3.3 \times 10^{-4}$.

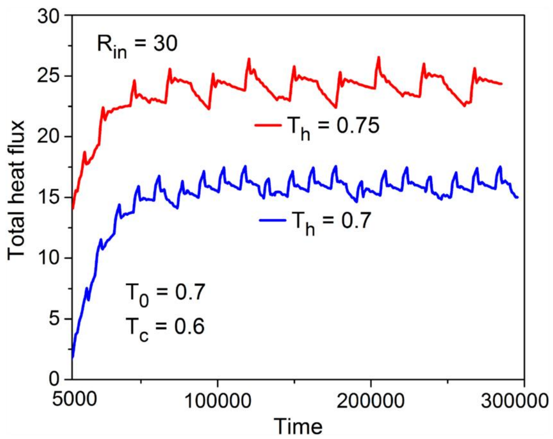

FIG. 5. (a) Time dependence of the heat flux Q for different heater temperatures $T_h = 0.7$ and 0.75. $2R_{in} = 60$, $\mathrm{Bo}_E^* = 2.5$, $u_2 \approx 3.3 \times 10^{-4}$.

cyclically, as well as the backflow of liquid. Both processes are controlled by the values of the film thicknesses h_1 and h_2. Without an electric field, the total heat flux is approximately $Q_0 \approx 14$. Thus, the action of the electric field and the backflow increase the heat flux by more than 1.7 times. Note that the film thickness at the condenser h_2 decreases when the flow of liquid starts, which leads to the enhanced evaporation of the film at the heater. This produces small oscillations of the film thickness h_1 superimposed upon its linear increase (blue curve in Fig. 4). The additional cause of oscillation is the generation of small waves in the film on the heater at the abrupt switch-on of the liquid inflow.

Numerical experiments with two different values of the heater temperature show that the average value of the total heat flux in the quasistationary regime is approximately proportional to the temperature difference between the heater and the condenser $\Delta T = T_h - T_c$ when other parameters remain unchanged (Fig. 5). It is worth noting that a further increase in the heater temperature leads to the film breakup at the heater due to more intense evaporation. The film thickness does not have time to recover, since the flow of liquid is a relatively slow process. In order to prevent the breakup, it is necessary to increase the minimum permitted film thickness. Moreover, the temperature of the condenser and the range of the film thickness at the condenser should be reduced in order to compensate for the increasing heat inflow.

Undoubtedly, the most interesting is the heat flux from the surface of the non-conductive inset. It was investigated in numerical experiments with different values of the half-width of the inset: $R_{in} = 30, 40,$ and 50 lattice units [Fig. 6(a)]. Sharp fronts on the curves correspond to the thinning of the film under the action of electric field. The heat flux from the inset increases with an increase in its width. The heat flux from a unit width of the inset is also calculated [Fig. 6(b)]. Interestingly, the average values of the heat flux per unit width are very close for different widths.

Thus, it is possible to realize a regular pulse action of a non-uniform electric field on the dielectric liquid film cooling a hot surface in order to increase the average value of the heat removal from the inset compared to the case without an electric field.

VI. CONCLUSION

We developed the mesoscopic numerical approach for simulating the fluid flow and heat transfer in a model of a heat pipe with the action of a non-uniform electric field on the fluid. The approach is based on the lattice Boltzmann method.

We demonstrate in a numerical experiment the possibility to realize the controlled quasiperiodic flow of an evaporating film of dielectric liquid in the vicinity of a non-conductive inset using the cyclic change of the electric field and the regularly switching flow of liquid condensed in the cold section back to the cooled surface. The action of a non-uniform electric field leads to a decrease in the thickness of the liquid film above the non-conductive inset, which leads to enhanced evaporation and an increase in the heat flux.

We simulate the process of the pulse action of a non-uniform electric field on the liquid film with a feedback based on the thickness of the liquid film at the cooling region and at the vapor condenser. Such combined action ensures an increased average value of the heat flux from the heater. In our experiments, the value of the heat flux is 1.7 times higher than the heat flux without the electric field for the

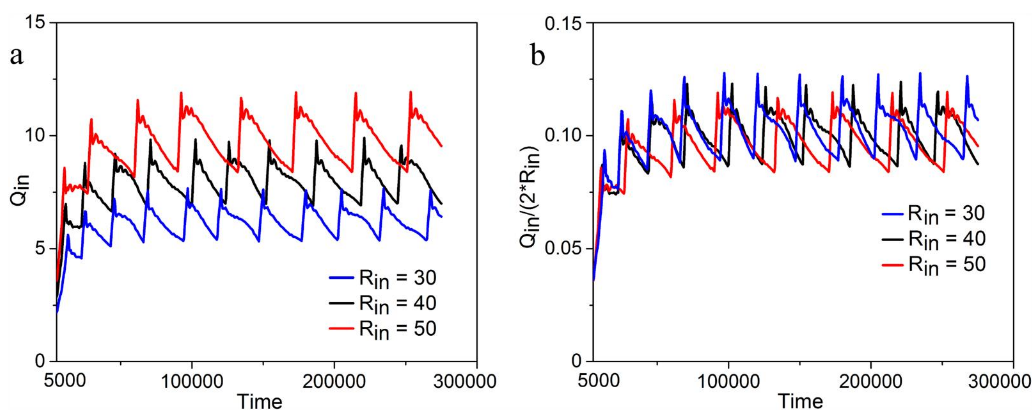

FIG. 6. (a) Time dependence of the heat flux from the surface of the non-conductive inset Q_{in}. (b) Time dependence of the heat flux from the unit width of the non-conductive inset $Q_{in}/2R_{in}$. Half-width of the inset is $R_{in} = 30, 40,$ and 50, $\mathrm{Bo}_E^* = 2.5, 4.4,$ and 6.9, correspondingly. $T_h = 0.75$.

same geometry of the region, the same temperatures, and the same amount of the cooling fluid.

Regimes of different temperatures of the cooling surface are investigated. For $T = 0.75$, the average heat flux is approximately 1.5 times higher than for $T = 0.7$. Further increase in the heater temperature, however, leads to a decrease in the cooling efficiency, to an increasing probability of the film rupture, and to a drastic fall of the heat flux.

We study the influence of the width of the non-conductive inset on the average heat flux from its surface. Calculations were carried out for three cases corresponding to the values of the modified electric Bond number (introduced in Sec. III) of 2.5, 4.4, and 6.9. An increase in the width leads to an increase in the total heat flux. At the same time, the average heat removal from a unit length remains approximately the same.

We demonstrate the feasibility of enhanced cooling of local regions of the hot surface by the intensification of the liquid film evaporation using the cyclic switching on and off of the non-uniform electric field.

ACKNOWLEDGMENTS

This work was supported by the Russian Science Foundation (Grant No. 25-29-00310), https://rscf.ru/en/project/25-29-00310/.

AUTHOR DECLARATIONS

Conflict of Interest

The authors have no conflicts to disclose.

Author Contributions

A. L. Kupershtokh: Conceptualization (equal); Investigation (equal); Methodology (equal); Software (equal); Validation (equal); Visualization (equal); Writing – original draft (equal). **D. A. Medvedev:** Conceptualization (equal); Investigation (equal); Methodology (equal); Software (equal); Validation (equal); Visualization (equal); Writing – original draft (equal). **A. V. Alyanov:** Software (equal); Validation (equal); Visualization (equal).

DATA AVAILABILITY

The data that support the findings of this study are available from the corresponding author upon reasonable request.

REFERENCES

[1] M. Potash and P. C. Wayner, "Evaporation from a two-dimensional extended meniscus," Int. J. Heat Mass Transfer **15**, 1851–1863 (1972).

[2] P. C. Wayner, "A dimensionless number for the contact line evaporative heat sink," J. Heat Transfer **111**, 813–815 (1989).

[3] A. D. Nazarov, A. F. Serov, V. I. Terekhov, and K. A. Sharov, "Experimental investigation of evaporative pulse-spray impingement coolings," J. Eng. Phys. Thermophys. **82**, 1184–1190 (2009).

[4] E. A. Chinnov, "Heat transfer enhancement and interaction of rivulets on the surface of a heated liquid film," High Temp. **61**, 559–564 (2023).

[5] R. S. Gaugler, U.S. Patent No. 2350348 (21 December 1942).

[6] G. M. Grover, T. P. Cotter, and G. F. Erickson, "Structures of very high thermal conductance," J. Appl. Phys. **35**, 1990–1991 (1964).

[7] Y. F. Gerasimov, F. Maidanik, G. T. Shchegolev, G. A. Filippov, L. G. Starikov, V. M. Kiseev, and Y. E. Dolgirev, "Low-temperature heat pipes with separate channels for vapor and liquid," J. Eng. Phys. **28**, 683–685 (1975).

[8] Y. F. Maydanik, "Loop heat pipes (review article)," Appl. Therm. Eng. **25**, 635–657 (2005).

[9] D. A. Reay, P. A. Kew, and R. J. McGlen, *Heat Pipes: Theory, Design and Applications*, 6th ed. (Elsevier, Oxford, UK, 2014)

[10] I. Marchuk, A. Karchevsky, A. Surtaev, and O. Kabov, "Heat flux at the surface of metal foil heater under evaporating sessile droplets," Int. J. Aerosp. Eng. **2015**, 391036.

[11] A. L. Karchevsky, I. V. Marchuk, and O. A. Kabov, "Calculation of the heat flux near the liquid-gas-solid contact line," Appl. Math. Modell. **40**, 1029–1037 (2016).

[12] M. J. Gibbons, C. M. Howe, P. Di Marco, and A. J. Robinson, "Local heat transfer to an evaporating sessile droplet in an electric field," J. Phys.: Conf. Ser. **745**, 032066 (2016).

[13] V. Vancauwenberghe, P. Di Marco, and D. Brutin, "Wetting and evaporation of a sessile drop under an external electric field: A review," Colloids Surf., A **432**, 50–56 (2013).

[14] V. S. Ajaev and O. A. Kabov, "Heat and mass transfer near contact lines on heated surfaces," Int. J. Heat Mass Transfer **108**, 918–932 (2017).

[15] V. V. Cheverda, A. L. Karchevsky, I. V. Marchuk, and O. A. Kabov, "Heat flux density in the region of droplet contact line on a horizontal surface of a thin heated foil," Thermophys. Aeromech. **24**, 803–806 (2017).

[16] A. L. Kupershtokh, D. A. Medvedev, and A. V. Alyanov, "Simulation of substrate cooling during evaporation of pure vapor from the surface of a thin film and liquid drops," J. Appl. Ind. Math. **17**, 582–591 (2023).

[17] A. L. Kupershtokh, D. A. Medvedev, and A. V. Alyanov, "Heat flux from the surface in the process of the rupture of a thin liquid film by an electric field," Phys. Fluids **35**, 102006 (2023).

[18] D. A. Medvedev and A. L. Kupershtokh, "Electric control of dielectric droplets and films," Phys. Fluids **33**, 122103 (2021).

[19] A. L. Kupershtokh and D. A. Medvedev, "Perforation of thin liquid films under the action of nonuniform electric field," J. Appl. Mech. Tech. Phys. **63**, 923–930 (2022).

[20] D. A. Medvedev and A. L. Kupershtokh, "Liquid dielectric films in a nonuniform electric field: Dynamics, perforation, and influence of electrode wettability," Interfacial Phenom. Heat Transfer **10**(2), 41–51 (2022).

[21] A. L. Kupershtokh, "Incorporating a body force term into the lattice Boltzmann equation," Vestn. Novosib. Gos. Univ., Ser.: Mat., Mekh., Inform. **4**, 75–96 (2004) (in Russian), see http://ancient.hydro.nsc.ru/sk/VESTNIK/Vestn-NGU-2004.pdf.

[22] A. L. Kupershtokh, "New method of incorporating a body force term into the lattice Boltzmann equation," in *Proceedings of the 5th International EHD Workshop* (University of Poitiers, Poitiers, France, 2004), pp. 241–246 http://ancient.hydro.nsc.ru/sk/EHD-2004/FR2004-LBE.pdf.

[23] A. L. Kupershtokh, D. A. Medvedev, and D. I. Karpov, "On equations of state in a lattice Boltzmann method," Comput. Math. Appl. **58**, 965–974 (2009).

[24] A. L. Kupershtokh, "Criterion of numerical instability of liquid state in LBE simulations," Comput. Math. Appl. **59**, 2236–2245 (2010).

[25] A. L. Kupershtokh, D. A. Medvedev, and I. I. Gribanov, "Thermal lattice Boltzmann method for multiphase flows," Phys. Rev. E **98**, 023308 (2018).

[26] A. L. Kupershtokh and D. A. Medvedev, "On contact wetting angles in the lattice Boltzmann method and their measurement," Eurasian J. Math. Comput. Appl. **12**, 84–91 (2024).

[27] Y. H. Qian, D. d'Humières, and P. Lallemand, "Lattice BGK models for Navier–Stokes equation," Europhys. Lett. **17**, 479–484 (1992).

[28] J. M. V. A. Koelman, "A simple lattice Boltzmann scheme for Navier–Stokes fluid flow," Europhys. Lett. **15**, 603–607 (1991).

[29] I. Ginzburg and P. M. Adler, "Boundary flow condition analysis for the three-dimensional lattice Boltzmann model," J. Phys. II Fr. **4**, 191–214 (1994).

[30] Y. Qian and S. Chen, "Finite size effects in lattice-BGK models," Int. J. Mod. Phys. C **8**, 763–771 (1997).

[31] L. D. Landau and E. M. Lifshitz, *Electrodynamics of Continuous Media* (Pergamon Press Inc., Oxford, 1984).

[32] A. L. Kupershtokh, "An evaporation flux of pure vapor in the method of lattice Boltzmann equations," J. Phys.: Conf. Ser. **2057**, 012070 (2021).

[33] A. L. Kupershtokh and A. V. Alyanov, "Evaporation and condensation of pure vapor at the liquid surface in the method of lattice Boltzmann equations," Numer. Methods Program **23**, 311–327 (2022) (in Russian).